ELSEVIER

Journal of Nuclear Materials 258–263 (1998) 1471–1475

journal of nuclear materials

Irradiation creep of vanadium-base alloys

H. Tsai [a,*], H. Matsui [b], M.C. Billone [a], R.V. Strain [a], D.L. Smith [a]

[a] *Argonne National Laboratory, Argonne, IL 60439, USA*
[b] *Institute of Materials Research, Tohoku University, Sendai 980-77, Japan*

Abstract

A study of irradiation creep in vanadium-base alloys is underway with experiments in the Advanced Test Reactor (ATR) and the High Flux Isotope Reactor (HFIR) in US. Test specimens are thin-wall sealed tubes with internal pressure loading. The results from the initial ATR irradiation at low temperature (200–300°C) to a neutron damage level of 4.7 dpa show creep rates ranging from ≈0 to 1.2×10^{-5}/dpa/MPa for a 500-kg heat of V–4Cr–4Ti alloy. These rates were generally lower than reported from a previous experiment in BR-10. Because both the attained neutron damage levels and the creep strains were low in the present study, however, these creep rates should be regarded as only preliminary. Substantially more testing is required before a data base on irradiation creep of vanadium alloys can be developed and used with confidence.

1. Introduction

Vanadium-base alloys are being developed as candidate materials for fusion first-wall/blanket structures because of their potential for low activation and attractive high-temperature properties [1,2]. While some of these properties have been extensively studied, irradiation creep, however, has not. Knowledge of irradiation creep is important because creep is a principal contributor to deformation and can potentially limit system performance.

Existing data on irradiation creep studies of vanadium-base alloy are extremely scarce. In one of the only two tests reported in the open literature, Vitek et al. [3] irradiated pressurized tubes made from a V–20Ti material in the fast reactor EBR-II to study, mainly, the effects of helium implantation on creep deformation. Helium atoms were injected in the middle section of the tubular specimens to 15 appm using a cyclotron before the irradiation, which was conducted at 700°C to a displacement-damage dose of 22 dpa. Postirradiation dimensional measurements were limited to two of the tubes. One tube, at a hoop stress of 34 MPa, showed a creep rate of $\approx 4 \times 10^{-5}$/dpa/MPa and no differences in creep rates between the base and helium-implanted materials. The other tube, at 39 MPa, showed a creep rate of $\approx 7 \times 10^{-5}$/dpa/MPa for the base material and a rate twice as high for the helium-implanted material. The extent of thermal creep, which could have contributed substantially to total creep because of the high test temperature, could not be discerned from the total creep in this experiment.

More recently, the creep behavior of a V–4Cr–4Ti material was studied in the BR-10 fast reactor at 445°C to a displacement damage of ≈3.0 dpa by Troyanov et al. [4]. The test specimen was a thin-wall tube and the applied stress was torsional. Thirteen deformation curves, at specimen stresses ranging from 17 to 164 MPa, were obtained. The results showed a creep rate of 5×10^{-6}/dpa/MPa for stresses up to ≈120 MPa, which was approximately one-half of the yield strength of the irradiated material. Above 120 MPa, the creep rate increased significantly.

Recognizing the importance of irradiation creep for vanadium-base alloys for fusion application, the US/Japan Jupiter collaboration program on fusion structural materials undertook a study of irradiation creep. In the first experiment, 10 pressurized-tube creep specimens were irradiated in the ATR-A1 experiment in the Advanced Test Reactor (ATR) [5]. The available results of this experiment are the subjects of this paper.

* Corresponding author. Tel.: +1 630 252 5176; fax: +1 630 252 9232; e-mail: htsai@anl.gov.

0022-3115/98/$19.00
PII: S0022-3115(98)00211-6

2. Experimental procedure

2.1. Creep tube fabrication

The creep specimens in the ATR-A1 experiments were pressurized tubes with welded end plugs. The tubes were prepared from two lots of materials: the 500-kg 832665 heat [6] with a V–4 wt% Cr–4 wt% Ti composition produced in US and the VM9407 laboratory heat with a V–4 wt% Fe–4 wt% Ti–0.1 wt% Si composition produced at Tohoku University in Japan. The 832665-heat tubes were produced by drawing, whereas and VM9407-heat tubes were produced by machining. All specimens had a nominal 4.57 mm outer diameter (OD), 0.25 mm wall thickness, and 25.4 mm length.

A US commercial vendor produced the 832665 tubing. The starting material was two 200-mm-long square bars cut from a 28.6-mm-thick warm-rolled plate. The bars, whose long dimensions paralleled the final rolling direction of the plate, were gun-drilled and machined into hollow cylinders with a 19.1-mm inner diameter (ID) and a 27.9-mm OD. Following cleaning and vacuum annealing (≈1025°C for 1 h in a vacuum of $\approx 7 \times 10^{-5}$ Torr), the two cylinders were drawn down at room temperature in three consecutive steps, each producing an areal reduction of ≈12–15%. After a total areal reduction of ≈40–45%, the pieces were cleaned, annealed, and drawn in three steps again. This cleaning/annealing/drawing process was repeated eight times to produce the finished tubing with a nominal 4.57 mm OD, 4.06 mm ID, and ≈45% cold work. To reduce the absorption of interstitial impurities during the vacuum annealing, the tubes were contained inside a pure Ti enclosure, which acted as the impurity getter. A total of ≈12 m of tube sections with various lengths was produced in this manner.

The drawn tubing has a fine grain microstructure with no apparent surface defects, as illustrated in Fig. 1. Sections of the drawn tubing were analyzed for their major alloying elements and interstitial impurity contents. The results indicated that the complex fabrication schedule caused only limited impurity uptake: oxygen content increased from 310 to 560 wppm, carbon from 80 to 300 wppm, and nitrogen from 85 to 95 wppm. These minor increases are not expected to substantially affect the properties of the material.

Because of the tubing's small size and the demanding flaw-detection specification (<0.025 mm flaw size), the drawn tubing could not be satisfactorily inspected with available ultrasonic or eddy current methods. Radiography was the only nondestructive means used to evaluate the internal condition of the tubing. A machined standard defect (0.025-mm-deep longitudinal groove) was included in the radiographs to establish the sensitivity of each exposure. Tube sections with questionable mass densities were excluded.

Before the attachment of the end caps, the 25.4-mm-long tube blanks were measured for their OD, ID, OD roundness, ID roundness, concentricity, and wall thickness with a coordinate measurement machine. The results of these measurements showed the dimensional attributes of the tube blanks to be excellent (all units in mm): ID 4.041 ± 0.002; OD of 4.569 ± 0.001; ID roundness 0.007 ± 0.003; OD roundness 0.005 ± 0.002; concentricity 0.007 ± 0.003; and wall thickness 0.264 ± 0.001.

2.2. Creep specimen fabrication

Ten creep specimens, eight with the 832665 heat material and two with the VM9407 heat material, were included in the ATR-A1 experiment. The circumferential plug-to-tube welds were made with an electron-beam welder in vacuum. Fig. 2 shows the microstructure of a

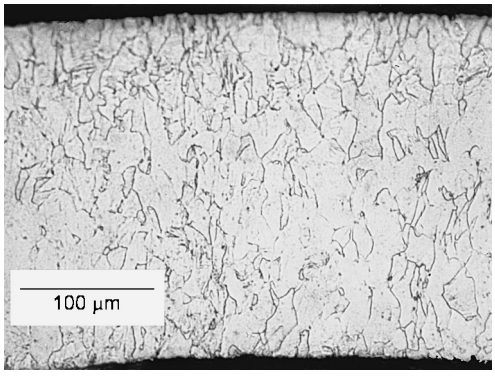

Fig. 1. Microstructure of drawn tube with 832665-heat V–4Cr–4Ti material.

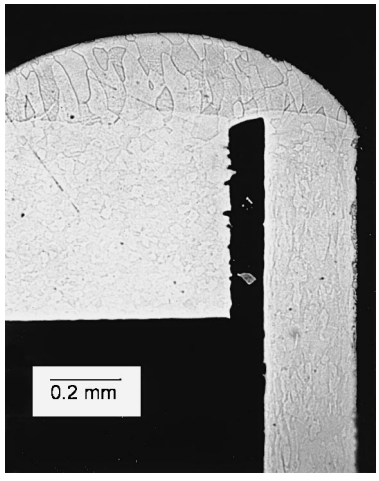

Fig. 2. Optical photomicrograph of specimen closure weld made with electron-beam welder.

typical weld. After the end plugs were attached, the assemblies were annealed at 1000°C for 1.0 h in vacuum while wrapped in a protective Ti getter foil. They were then pressurized to the desired level, through a 0.25-mm-dia. hole in the top end plug, with high-purity helium in a pressure chamber. Two of the 832665 specimens were designated as stress-free swelling controls and were therefore not pressurized. The final closure weld of the 0.25-mm-dia. hole was made with a laser through the quartz window in the pressure chamber. The specified pressure loading was determined with a code that accounted for thermal expansion of the vanadium alloy tubing, compressibility of the helium gas, and anticipated specimen temperature. Following the leak check and visual inspection, the dimensions of the assembled creep specimens were measured with a precision laser profilometer. The measurements were made at 5 axial locations (x/l of 0.1, 0.3, 0.5, 0.7 and 0.9) at every 9° azimuthal interval, and the 19 azimuthal readings were averaged to yield the mean diameter for each axial location.

2.3. Irradiation conditions

The ATR-A1 experiment consisted of 15 stacked, lithium-bonded subcapsules spanning the 1210 mm core height. The 10 creep specimens were each contained in a subcapsule to preclude interactions should any one rupture unexpectedly. To reduce the atypical transmutation of V into Cr due to the reactor's thermal flux, a neutron filter made of Gd was installed in each subcapsule. The duration of the irradiation was 132.9 effective-full-power days. The experiment had two target temperatures: 200 and 300°C. However, because of the space limitation and axial flux gradient, the achieved displacement damage and specimen temperatures were not uniform, particularly for the nominally 200°C specimens. The calculated dpa, temperature, and stress loading for the specimens are shown in Table 1. For specimens A11 and A3, the calculated effective stress of 172 and 196 MPa were quite high, reaching ≈90 and 97% of the reported yield strength of the nonirradiated material [7].

3. Experimental results

The first step in the postirradiation examination was to determine specimen integrity by puncturing the subcapsules containing the specimens and measuring the subcapsule plenum pressure. The results showed no abnormal pressure, implying that all pressurized specimens were intact. This positive finding was later confirmed by visual inspection of the specimens after they were retrieved from the subcapsules.

Diameter measurements have been completed for the eight 832665 specimens with V–4Cr–4Ti material. Measurements for the two VM9407 specimens with V–4Fe–4Ti–0.1Si material have been deferred due to the facility modification required to accommodate the higher gamma activities in these two specimens induced by the irradiation.

In calculating the effective strains for the 832665-heat specimens the averaged diameters were determined with the laser profilometer in the same manner as before the irradiation. To preclude end effects, only the three middle-diameter measurements of the specimen were used to calculate the average diametral strain. For the two zero-stress specimens for the 200 and 300°C groups, the diametral strains were small (0.05% and 0.11%), respectively, indicating insignificant density changes under the conditions irradiated. The precision of the profilometry measurements is ≈0.5 μm, or ≈0.01% in strain. To facilitate a general stress analysis, the specimen's

Table 1
Effective stress in ATR-A1 creep specimens

Target temperature (°C)	Specimen no.	Material [a]	Calculated temperature (°C)	Calculated damage (dpa)	Effective [b] stress (MPa)
300	A1	832665	286	4.3	0
	A10	832665	302	4.6	87
	A7	832665	300	4.7	129
	A11	832665	295	4.5	172
	J2	VM9407	300	4.1	163
200	A5	832665	144	0.7	0
	A4	832665	213	1.5	88
	A2	832665	234	3.5	130
	A3	832665	259	3.9	196
	J3	VM9407	212	3.0	165

[a] Heat 832665: nominal composition V–4 wt% Cr-4wt%Ti; Heat VM9407: nominal composition V–4wt% Fe–4wt%Ti–0.1wt%Si.
[b] Effective von Mises stress [8].

internal pressure loading and the measured diametral strain were converted to the wall-averaged effective von Mises stress and effective strain according to the following formulas [8].

$$\sigma_e = (0.5)(3)^{0.5}(r_m/t)\Delta P,$$

$$\varepsilon_e^C = 2(3)^{-0.5}(r_o/r_i)(\varepsilon_{dia}^C),$$

where σ_e is the effective stress, r_i, r_m, r_o are the internal, midwall, and external radii, respectively, t is the wall thickness, ΔP is the difference in internal and external gas pressure at temperature, ε_e^C is the effective creep strain, and $\varepsilon_{dia}^C = (\varepsilon_{dia}^C - \varepsilon_e^{stress\text{-}free})$ is the component of the measured OD hoop strain associated with creep. To obtain the creep coefficient (A), the assumed form of the irradiation creep law is

$$\varepsilon_e^C = A\sigma_e D,$$

where D is the neutron damage in dpa. The resultant effective creep strains and creep coefficients are summarized in Table 2.

4. Discussion

Vanadium-base alloys have a propensity to absorb interstitial impurities at elevated temperatures and become embrittled. The production of the drawn creep tubing for this study was particularly challenging because of the tubing's large surface-to-volume ratio and the significant number of process steps involved. The successful production of these tubes, by a commercial vendor to a set of tight tolerance specifications, indicates that vanadium-base alloys can be satisfactorily processed if reasonable process control is implemented.

The irradiation creep data from this study, along with the Troyanov et al. data [4] from a 445°C irradiation experiment conducted in BR-10, form a preliminary data set for evaluating the irradiation creep of V–4Cr–4Ti alloy. This data set is shown in Fig. 3. In the present study, because the attained neutron damage levels were low, the measured strains small, and the number of test specimens limited, the uncertainties on strain rates were probably high. These uncertainties are expected to diminish when additional data from tests currently underway or being planned for the HFIR become available. The J2 and J3 specimens from the present study, when evaluated, will provide a performance comparison between the V–4Cr–4Ti and V–4Fe–4Ti–0.1Si materials.

The data from the present study indicate strain rates generally lower than those measured by Troyanov et al., as shown in Fig. 3. The Troyanov et al. data also display a bilinear stress dependence: at stress greater than ≈120 MPa, which is approximately one-half of the yield strength of the irradiated alloy, the creep rate increases sharply. This bilinear dependence, however, could not be substantiated in the present study due to the limited data. Troyanov et al. noted that such threshold-type creep acceleration had been observed previously on stainless steel materials in experiments in the BR-10 reactor. But in comparison with the stainless steels, the acceleration threshold for the V–4Cr–4Ti alloy occurs at significantly lower stress with respect to the yield point. Recently, Grossbeck et al. [9] reported similar nonlinear stress dependence for a bcc alloy HT9 (a tempered martensitic steel) at elevated temperatures; they attributed the abrupt rate increase to the domination of a preferred absorption glide mechanism. Determination whether this bilinear behavior exists for vanadium-base alloy is an important objective for future irradiation creep experiments.

5. Conclusions

An experiment on irradiation creep of vanadium-base alloys with pressurized-tube specimens was recently completed in the ATR at low temperatures (≈200–300°C) to ≈4.7 dpa. Two materials were studied: a V–4Cr–4Ti alloy (Heat 832665) produced in US and a V–4Fe–4Ti–0.1Si alloy (Heat VM9407) produced at Tohoku University in Japan. The peak effective stress loading in the specimens was ≈200 MPa. None of the specimens ruptured during the irradiation. The measured strain rates,

Table 2
Summary creep data for 832665-heat material in ATR-A1 experiment

Specimen	Temperature (°C)	Damage (dpa)	Average σ_e (MPa)	Average ε_{dia} (%)	Average ε_e^C (%)	Creep coef. ($dpa^{-1}MPa^{-1}$)
A1	286	4.3	0	0.11	–	–
A10	302	4.6	87	0.10	≈0	≈0
A7	300	4.7	129	0.28	0.22	3.6×10^{-6}
A11	295	4.5	172	0.79	0.89	11.5×10^{-6}
A5	144	0.7	0	0.05	–	–
A4	213	1.5	88	0.16	0.14	11.0×10^{-6}
A2	234	3.5	130	0.05	≈0	≈0
A3	259	3.9	196	0.13	0.10	1.4×10^{-6}

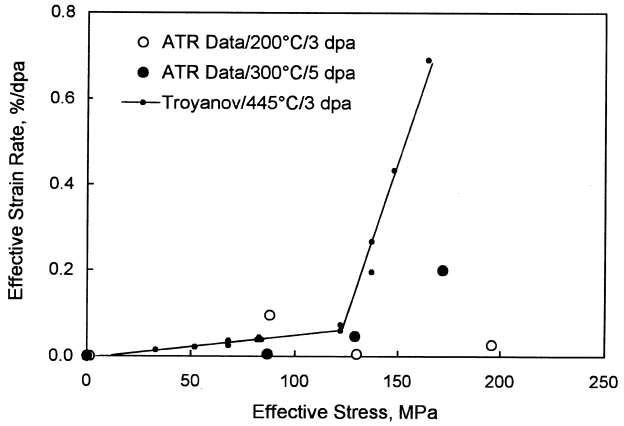

Fig. 3. Data set of effective strain rate from ATR experiment and torsional creep tests in BR-10 by Troyanov et al. [4]. Correlation given by Troyanov (solid line) shows bilinear stress dependence.

ranging from 0 to 12×10^{-6}/dpa/MPa for the 832665 heat alloy, were generally lower than reported by Troyanov et al. The creep rates for the VM9407 heat specimens have not yet been measured. Within the limitation of the data from the present study, no abrupt acceleration of creep rates at high stress levels, as reported by Troyanov et al., could be substantiated.

References

[1] D.L. Smith et al., Fusion Engineering and Design 29 (1995) 399.
[2] D.L. Smith et al., J. Nucl. Mater. 233–237 (1996) 356.
[3] J.M. Vitek et al., J. Nucl. Mater. 141–143 (1986) 982.
[4] V.M. Troyanov et al., J. Nucl. Mater. 233–237 (1996) 381.
[5] J.W. Rogers et al., Neutron Spectrum Studies in the ATR, 7th ASTM – Euratom Symposium on Reactor Dosimetry, Strasbourg, France, 1990.
[6] H.M. Chung et al., Fusion Reactor Materials Semiannual Progress Report, DOE/ER-0313/17, Oak Ridge National Laboratory, Oak Ridge, TN, 1995, pp. 5–11.
[7] M.C. Billone et al., these Proceedings.
[8] E.R. Gilbert, L.D. Blackburn, J. Eng. Mater. Tech. ASME Trans. (1977) 168.
[9] M.L. Grossbeck et al., Effects of Radiation on Materials, 18th International Symposium, ASTM STP 1325 (1997).